

Numerical investigation of inert and reactive spray characteristics during pilot injection of a dual fuel injector

Jens Frühhaber^{1*}, Andreas Peter², Sebastian Schuh³, Thomas Lauer¹, Michael Wensing², Franz Winter³, Peter Priesching⁴, Klaus Pachler⁴

¹ Institute for Powertrains and Automotive Technology, Technische Universität Wien
Getreidemarkt 9, 1060 Vienna, Austria
jens.fruehhaber@ifa.tuwien.ac.at, thomas.lauer@ifa.tuwien.ac.at, www.ifa.tuwien.ac.at

² Institute of Engineering Thermodynamics, FAU Erlangen-Nuremberg
Am Weichselgarten 8, 91058 Erlangen, Germany
andreas.peter@fau.de, michael.wensing@fau.de, www.ltt.uni-erlangen.de

³ Institute of Chemical, Environmental and Bioscience Engineering, Technische Universität Wien
Getreidemarkt 9, 1060 Vienna, Austria
sebastian.schuh@tuwien.ac.at, franz.winter@tuwien.ac.at, www.vt.tuwien.ac.at

⁴ AVL List GmbH
Hans-List-Platz 1, 8020 Graz, Austria
peter.priesching@avl.com, klaus.pachler@avl.com, www.avl.com

Key words: CFD, Dual Fuel, Spray Characteristics, Combustion Process

Abstract. Dual fuel combustion will become more important in the field of maritime propulsion, due to the introduction of the so called Emission Controlled Areas within the IMO Tier III legislation. To meet the stringent emission targets, ships propelled with HFO may switch to dual fuel operation mode in the protected areas. The combustion process is characterized by the injection of a small amount of fuel oil, which ignites a premixed natural gas-air mixture. The resulting short injection durations oblige the injector into the ballistic working regime. This influences spray penetration, mixture formation and ignition behavior.

In the present work, a CFD model of a dual fuel injector was developed using the commercial code AVL FIRE[®]. Due to the ballistic working regime, the main challenge for the modeling is to capture the opening and closing behavior of the injector. Therefore, optical investigations were carried out in an injection bomb to characterize the liquid and the vapor phase at an early stage of spray propagation. Based on the experimental observations, a methodology assuming constant momentum along the spray axis was applied to estimate the initial penetration velocities. The injection profile is adjusted for different fuel quantities to investigate the resulting spray characteristics. To realize the observed dependencies of the spray penetration from chamber conditions in simulation and to depict the decrease of liquid length after the end of injection, a suitable initial droplet spectrum was defined. The developed model is able to predict the experimental observed penetration and contour of the spray plume.

The spray model is extended by a detailed reaction mechanism to simulate the combustion process of the diesel jet. The ignition delay was validated using measurements of the OH*

emission of the flame. Measured OH* intensities enable a detailed characterization of the development and the propagation of the first flame structures. The distribution of the simulated OH concentration shows a good correlation with the experimental data concerning the contour and the penetration behavior of the flame.

1 INTRODUCTION

Emission thresholds and fuel efficiency are the main driving forces for the development of next generation internal combustion engines. Even the transportation sector is strongly affected by stricter legal requirements. The maritime industry, for example, has to comply with the regulations introduced by the IMO in the framework of the Tier III, which is actually valid in the so call Emission Controlled Areas. The Tier III strictly limits the emission of nitrogen oxides and the sulfur content of the fuel. Additionally an Energy-Efficiency Design Index is established to reduce the emissions of greenhouse gases [1],[2]. Both, the emissions of pollutants and greenhouse gases, can be reduced using the dual fuel combustion of natural gas and diesel. Thereby, less nitrogen oxides are formed due to the lean combustion in the gas mixture, while the high hydrogen to carbon ratio of methane diminishes the greenhouse gas emissions. Dual fuel engines enable an appropriate reaction on the local availability of LNG due to their fuel flexibility. The engine may also operate in the dual fuel mode within the ECAs, while it switches to pure diesel operation outside this areas [3][4].

The dual fuel combustion process is initialized by a pilot injection of fuel oil that ignites a lean natural gas-air mixture. The combination of diffusive combustion, known from CI engines and premixed combustion, known from SI engines results in a very complex process. Depending on the operating point, the process is limited due to the occurrence of flame quenching in very lean mixtures and knocking for high diesel substitution rates [5].

The engines operating range may include different diesel shares from < 1% to up to 100% resulting in a demand on a flexible injection system, which is able to exactly provide the requested fuel amount for every operating point. Particularly for small fuel amounts, that oblige the injector in the ballistic working regime, a high influence on the spray characteristics is recognizable. This influence was investigated by the authors in [6] with a wide range dual fuel injector using Mie-scattering and Schlieren-imaging technique. The investigations show asymmetric spray patterns and shot-to-shot variations, which are mainly caused by the ballistic working regime of the injector. In this regime the ballistic movement of the needle leads to transient conditions at the nozzle exit, which depicts a challenge for the modeling of the injection process in the CFD. To overcome this issue the approach of the authors in [7] is to introduce an unsteady nozzle diameter to adjust the initial velocity of the fuel droplets. However, the determination of the transient injection parameters and the correct modeling of the liquid phase represent the key task to describe the pilot injection process using CFD.

In the present work the modeling of a dual fuel injector is presented to investigate the influence of transient injection parameters on spray propagation and mixture formation. The model is validated with experimental data from a combustion vessel. Further on, the ignition and the combustion of the pilot jet is studied using a detailed reaction scheme.

2 EXPERIMENTAL SETUP

The spray characteristics were investigated in the optically accessible combustion vessel described in detail by the authors in [8]. The vessel consists of five windows with a diameter of 125 mm to ensure optical accessibility from each side and from the top. The investigated seven-hole dual fuel injector is mounted in the injector slot at the bottom. The nozzle holes with a diameter of 280 μm are uniformly distributed and form a spray umbrella of 145 deg. The injection parameters and the ambient conditions used within the measurement program are shown in Table 1.

Table 1: Injection parameters and ambient conditions in the vessel

Pressure [MPa]	6 - 9
Temperature [K]	823 - 973
Injection Pressure [MPa]	100
Injected Mass [mg]	34 - 88
Fuel Temperature [K]	333

The liquid phase of the spray is measured using Mie-scattering technique, which is based on the elastic scattering of light at the surface of liquid droplets. Stroboscopic flash lamps (Drello HL4090) illuminate the chamber via the side windows, while a CCD camera (PCO Sensicam) detects the scattered light via the top window. The vapor phase of the spray is recorded using Schlieren-imaging technique. Schlieren-imaging is based on the diffraction of collimated light beams at optical inhomogeneity caused by density gradients or different thermodynamic conditions. A LED-Array (Hardsoft IL-106G) emits collimated light that passes the combustion vessel from the top to the bottom, where it is reflected at a mirror amounting around the injector tip. The reflected light is focused on a Schlieren knife edge that blocks diffracted light resulting in a phase contrast image of the spray, which is recorded by a high-speed camera (Photron SA-Z). The detailed measurement procedure and the evaluation of the geometrical properties of the spray plumes is described in [8].

For the characterization of the combustion, an iCCD camera is used to record the OH* emission that is detectable at a wavelength of 308 nm and indicates regions of premixed combustion. The probability of the first OH* signal is evaluated to determine the ignition delay time due to the large amount of premixed fuel that ignites immediately at the SOC using the methodology developed by Riess [9].

3 MODELING APPROACH

3.1 Computational Mesh and Solver Setup

The spray modeling is carried out on a simplified cylindrical spraybox mesh using the commercial CFD code AVL FIRE[®]. On this mesh the spray propagation of a single jet is studied. The dimensions of the cylindrical box, 120 mm in length and 40 mm in width, are chosen to avoid influences from the boundaries. The boundaries are modeled as walls with a fixed temperature, except the boundary opposite the nozzle, which is modeled as a non-reflecting outlet. The mesh consists of hexahedral cells with a size of 1 mm and is partially

refined in the spray center axis. Figure 1 illustrates a cut through the centerline of the computational mesh to demonstrate the local mesh structures.

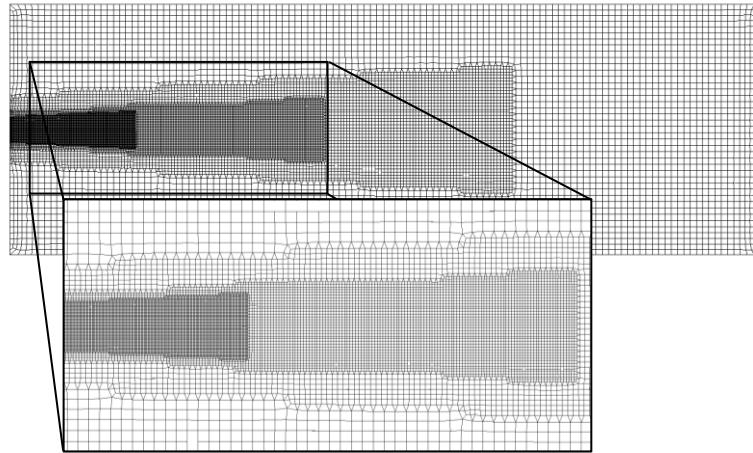


Figure 1: Cut through computational mesh with local refinements

Three refinement levels are used starting with a cell size of $125\ \mu\text{m}$ in the vicinity of the nozzle to provide a suitable spatial resolution leading to a total mesh size of about 700,000 cells. The conical shape of the refinements captures the spreading of the spray in radial direction with increasing distance from the nozzle. The associated dimensions of the refinements are listed in Table 2.

Table 2: Geometrical dimensions of the mesh refinements

Refinement	L [mm]	R1 [mm]	R2 [mm]	Cell size [μm]
1	80	5	10	500
2	50	3	5	250
3	20	2	3	125

The small cell size in the vicinity of the nozzle is chosen to ensure a correct description of the momentum exchange between the droplets and the surrounding air. For high injection velocities, typical for high pressure injection events, in combination with small cell sizes short time steps are needed to comply with the requirement of low courant numbers to provide numerical accuracy. Therefore, the time step during the injection process is set to $1\ \mu\text{s}$ and is followed by $2.5\ \mu\text{s}$ at the end of injection to observe the vapor phase. A RANS approach using the $k\text{-}\zeta\text{-}f$ turbulence model, implemented in AVL FIRE[®], is selected to calculate the turbulent flow introduced by the injection process. Further on, a large eddy simulation (LES) is carried out, which directly resolves the larger turbulent structures, to evaluate the influence of the turbulence on mixture formation. As LES only captures larger turbulent structures depending on the temporal and spatial resolution, the so called sub-grid scales still have to be modeled. In this work a Coherent Structure model implemented in AVL FIRE[®] is used to model the sub-grid turbulence [10]. To fulfill the requirement of a courant number smaller one for LES, the time step during injection is set to $0.5\ \mu\text{s}$. The LES is performed on the computational mesh depicted in Figure 1, which already provides a fine spatial resolution in the spray area. Also

finer mesh resolutions are used for LES as shown by the authors in [11]. As the present model will serve as a basis for an engine model later on, further refinement is not implemented to keep the computational effort within a feasible range.

3.2 Modeling the Pilot Injection

The liquid phase of the spray is depicted using a discrete droplet approach, whereby a statistically sufficient number of parcels is introduced at every time step during injection. These parcels consist of a certain number of identical, non-interacting droplets, which are tracked through the simulation domain in a Lagrangian manner. Their trajectories are determined by the force acting on the droplets, which is in the case of fuel sprays mainly influenced by the drag force F_D described by Equation 1 [12].

$$\rho_l V_d \vec{F}_D = \frac{1}{2} \rho_g C_d A_d * |\vec{u} - \vec{v}| * (\vec{u} - \vec{v}) \quad (1)$$

The droplet evaporation is described by the approach of Dukowicz [13], while the breakup phenomena are simulated using the Wave breakup model. The Wave model is derived from the theory of growing oscillations on the droplet surface, which are a result of high relative velocities between the droplet and the surrounding gas. The wavelength Λ and the growth rate Ω , mainly influenced by the physical properties of the liquid fuel and the surrounding gas, determine the radius r of the stable product drop and its characteristic breakup time τ described by Equation 2 and 3. Additionally, two model constants B_0 and B_1 are available to adjust the breakup process [14].

$$r = B_0 * \Lambda \quad (2)$$

$$\tau = \frac{3.726 B_1 r}{\Lambda \Omega} \quad (3)$$

The injection parameters depict an important factor, which need to be defined to model the spray propagation. In the case of pilot injections, the short injection durations result in a very transient behavior of the mass flow and the initial velocity at the nozzle exit due to the ballistic needle movement. Based on the temporal evolution of the spray plume, known from the measured Schlieren images, a methodology of momentum conservation [15], [16] is applied to calculate the initial velocity in the vicinity of the nozzle. Starting from Equation 4, describing the momentum flux \dot{M} at the spray root and Equation 5 the momentum flux at an arbitrary position x downstream the nozzle, Equation 6 is derived to calculate the initial velocity v_0 .

$$\dot{M} = \rho_D A_n v_0^2 \quad (4)$$

$$\dot{M}(x) = \rho_g v^2 \pi x^2 \tan^2 \left(\frac{\alpha}{2} \right) \quad (5)$$

$$v_0 = \frac{x^2}{t} * a * \tan \left(\frac{\theta}{2} \right) * \sqrt{\frac{\rho_M}{\rho_D * d^2 * \sqrt{C_A}}} \quad (6)$$

Hereby, the contraction coefficient C_A is introduced taking into account the reduction of the free flow area caused by non-uniform velocity profiles, hydraulic flip or cavitation. The constant a relates the measured cone angle Θ to the theoretic angle α used in Equation 5. According to Naber and Siebers [15] a value of 0.66 is suitable to achieve a good correlation between simulation results and experimental data. The mixture density ρ_M considers the amount of diesel fuel in the spray plume and is used instead of the density of the ambient gas ρ_g . Assuming a value of 0.9 for the contraction coefficient, Equation 6 is applied to calculate the initial velocity from the experimentally observed spray characteristics. Figure 2 depicts the calculated velocities over time after SOI for the single measurements and their associated mean value. As the velocity is known, the velocity coefficient C_V , which relates the observed velocity to the theoretic Bernoulli velocity, can be calculated. The velocity and the contraction coefficient are used to estimate the maximum mass flow rate \dot{m}_D during injection according to Equation 7.

$$\dot{m}_D = C_A C_V A_n \sqrt{2\rho_D \Delta p} \quad (8)$$

The knowledge of the maximum mass flow rate is necessary to define a suitable injection profile due to the fact that it strongly varies with the injection duration in the ballistic working regime. Figure 2 illustrates two simplified injection profiles derived from the maximum mass flow rate and the slope during opening and closing event of the injector known from an injection rate measurement.

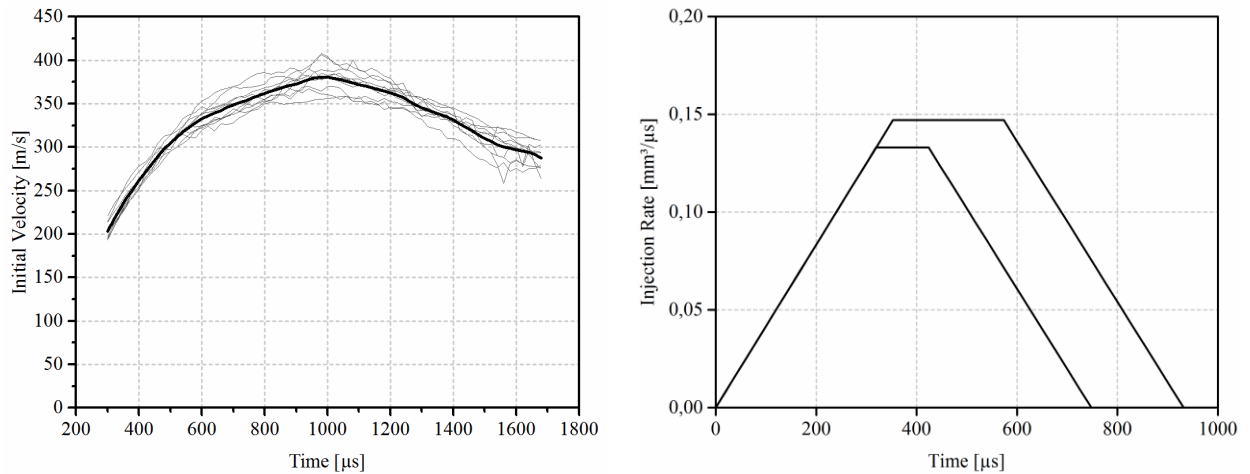


Figure 2: Calculated initial velocity (left) and simplified injection profiles (right)

Further on, an initial droplet spectrum is empirically imprinted on the introduced parcels to depict the experimental observed dependencies of the liquid penetration from temperature. This methodology is chosen instead of the wide spread blob injection approach, whereby the nozzle diameter determines the initial droplet size, to overcome the problem of slow droplets initialized during injector closing. These droplets hardly evaporate due to the inhibited breakup caused by very low relative velocities. This results in a higher penetration of the

liquid droplets than experimentally observed. A correlation between the simulated and the measured penetration of the liquid phase could be achieved using an initial SMD of 20 μm .

3.3 Modeling the Combustion

The ignition and the combustion is modeled using a detailed reaction mechanism, which is able to handle both diesel and dual fuel combustion. This methodology is necessary, because the generated spray model will serve as a basis for a model of a dual fuel research engine later on. Thereby, the kinetically controlled processes of knocking and flame quenching will be investigated using the detailed reaction chemistry. However, the mechanism is integrated into AVL FIRE[®] via the general gas phase reaction module that solves a homogeneous reactor model for every computational cell at every time step. The integrated multi zone model is used to reduce the computational time by a clustering of cells with similar conditions [17].

Diesel fuel consists of a variety of different components that cannot be captured by a mechanism entirely. Therefore, a surrogate fuel for diesel has to be defined. Usually n-heptane is used as surrogate [7], [17], because of its comparable chemical properties. The problem that the physical properties of n-heptane strongly differ from diesel fuel, and therefore strongly influence evaporation and breakup of the fuel droplets, can be overcome by imprinting the averaged physical properties of diesel on the liquid phase, while the vapor phase is treated as n-heptane. Applying this methodology, n-heptane chemistry can be implemented to calculate the gas phase reactions.

4 RESULTS

4.1 Spray Propagation

The simulation model is applied to study the influence of the ambient conditions, depicted in Table 1, on the spray propagation. The simulated penetration length of the liquid phase is described by the distance from the nozzle exit up to the mass average of the 1 % furthest parcels. The vapor penetration is depicted in the CFD code as distance to the furthest computational cell containing 0.001 kg/kg vaporous fuel. Simulated liquid and vapor penetration length are compared with the experiments by evaluating the furthest position at which Mie and respectively Schlieren signal is detectable. Figure 3 illustrates the penetration length of the spray for an ambient pressure of 60 bar and an ambient temperature of 650 °C on the left side. Additionally, the contours of the spray are plotted at 500 μs and 900 μs after the start of injection (ASOI), while the left side represents the measured Schlieren signal intensity and the right side depicts the simulated fuel mass fraction bounded by a value of 0.001 kg/kg. For both, the liquid and the vapor phase, the simulation results are in good agreement with the experimental data. Even the decrease of the liquid penetration during the closing event of the injector after 800 μs is captured by the model. For the vapor phase a retarding of the penetration velocity with increasing distance from the nozzle is observed. On the one hand, this behavior is caused by the increasing radial dispersion of the momentum flux. On the other hand there is a very transient momentum flux due to the ballistic movement of the injector needle that strongly influences the penetration behavior. Further on, the vapor penetration is reduced with an increasing ambient pressure depicted on the right side of Figure 3. This observation is caused by the increase of the ambient density from 22.2 kg/m³ to 33.0 kg/m³ for a pressure increase

from 60 bar to 90 bar. The effect of the ambient density on vapor penetration is also discussed in [15], [16].

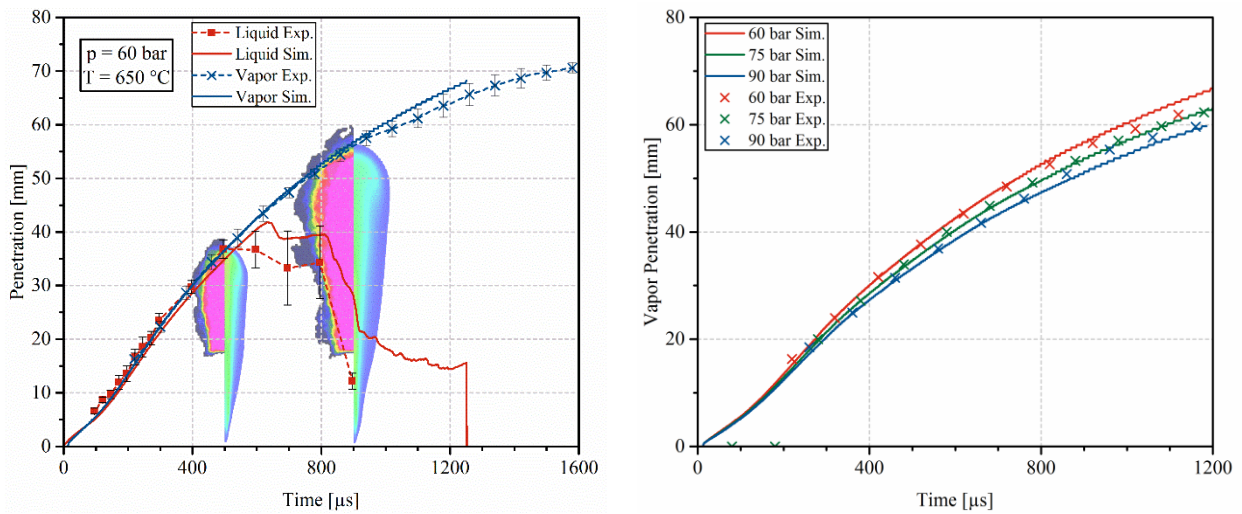


Figure 3: Simulated and measured spray penetration and contour for $p = 60$ bar and $T = 650$ °C (left); vapor penetration for different ambient pressures (right)

To evaluate the influence of the turbulence treatment in the CFD code on the local mixture formation in the spray plume, the RANS results are compared with a single representative injection event modeled with LES. Figure 4 illustrates the calculated distribution of the vaporous fuel inside the spray plume for LES on the left side and for RANS on the right side at three different temporal positions (ASOI).

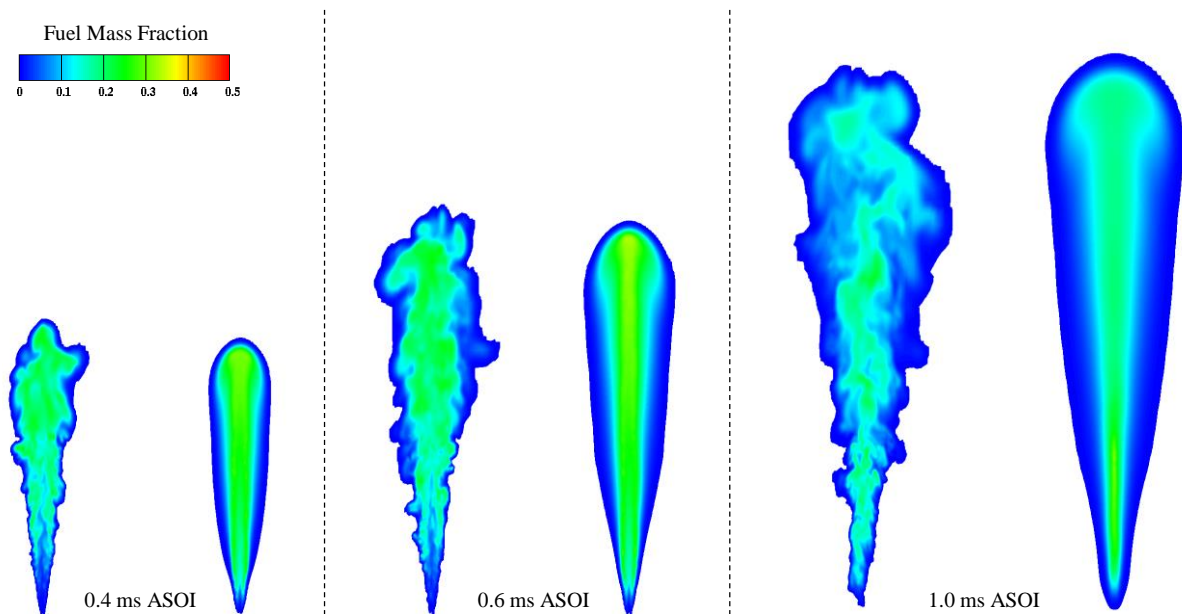


Figure 4: Simulated fuel mass fraction using LES (left) and RANS (right) for different temporal positions ASOI

While the RANS results show a symmetric distribution of the fuel mass that is only dependent from the axial and radial distance from the nozzle, the LES results depict an asymmetrical distribution characterized by many recirculation areas. This observation is mainly caused by the direct resolution of larger turbulence structures by the LES. Therefore, the LES may be suitable to study the influence of small variations of the injection parameters on the turbulent mixture formation induced by a single jet.

4.2 Ignition and Combustion

In this section, the simulated ignition delay and the flame propagation are compared with the experimental derived OH* signal. The ignition delay is evaluated determining the elapsed time between SOI and the maximum temperature gradient in the simulation domain, while the experimental observed ignition delay is evaluated using the methodology of Riess [9] described above. Figure 5 illustrates the simulated and measured ignition delay as a function of temperature (left) and pressure (right). From 550 °C to 650 °C ambient temperature, a rapid decrease of the ignition delay time is recognizable, while the decrease between 650 °C and 700 °C is quite lower. This behavior can be explained by the entering of the NTC regime in this temperature range, which is a commonly known phenomena for higher hydrocarbons. The model predicts a shorter ignition delay at 550 °C as experimentally observed, while there is a good agreement for higher temperatures. An increasing ambient pressure results in shorter ignition delay times. This influence is more significant for the experimental data in comparison with the simulations, which could be caused by an underestimation of the entrainment of hot air in the spray plume leading to slower evaporation of the droplets. However, there is good correlation for higher pressures occurring in DF engines.

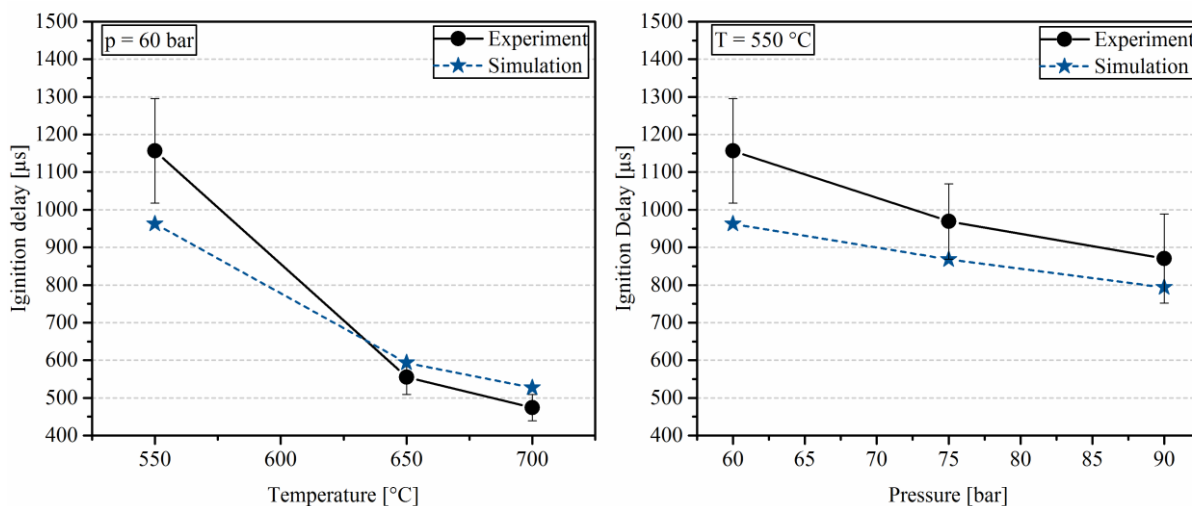


Figure 5: Simulated and measured ignition delay as function of temperature (left) and pressure (right)

Another important factor for the modeling of the combustion is the correct prediction of the establishment of the first flame structures and their propagation through the combustion chamber. Therefore, the simulated OH mass fraction, bounded by a value of 0.0001 kg/kg, is compared with a tomographic reconstruction of the measured OH* signal in Figure 6.

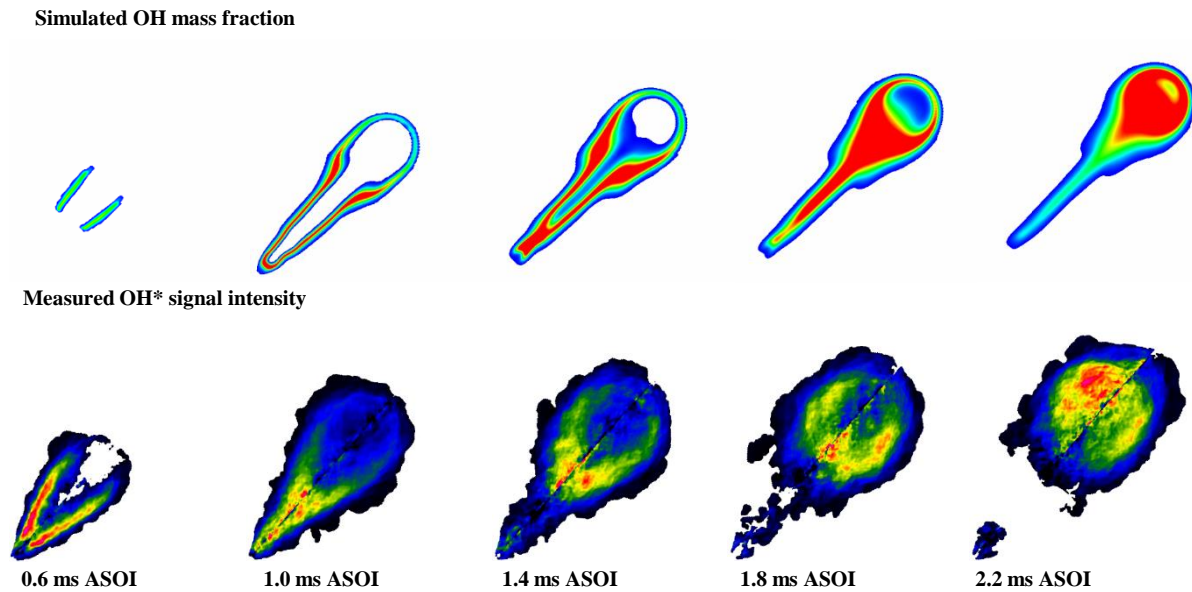


Figure 6: Simulated OH mass fraction (top) compared with measured OH* signal intensity (bottom) for $p = 60$ bar and $T = 700$ °C

The flame contours are depicted for five temporal positions after SOI, while the simulation results are situated in the top row. The experimental data is illustrated below. The injector nozzle is situated in the bottom left corner of the single pictures. In the first picture the spray ignites at the borders close to the nozzle due to the high air entrainment in this area enabling a fast evaporation that is needed to form an ignitable mixture. In the following, the flame starts to spread along the spray borders before it moves towards the centerline of the spray after the end of injection. Later on, the flame detaches and starts to move away from the nozzle, while there is still a region close to the spray tip where no flame structures are ascertainable. In the last picture the flame reaches the spray tip and forms a spherical structure, which moves away from the nozzle. The model predicts the experimental observed behavior of the flame and is therefore suitable to simulate the combustion of pilot jet in a dual fuel engine.

5 CONCLUSIONS AND OUTLOOK

In the present work numerical investigations were carried out to study the spray propagation and the combustion of a pilot injection process. The developed CFD model is able to predict the experimental observed penetration of the liquid and the vapor phase in a combustion vessel. The used methodology to determine a transient initial velocity profile of the droplets during the injection event was found to be suitable to depict the penetration behavior of the vapor phase. Further on, the influence of an increasing ambient density on the vapor penetration is captured by the model. The approach to empirically imprint a droplet spectrum on the initial droplets is able to describe the observed retarding of the liquid penetration during the injector closing event.

By the application of a detailed reaction mechanism to model the ignition and the combustion, a good correlation for the experimental observed ignition delay time and the flame propagation could be achieved. Even the first ignition zones are depicted accurately by the

mechanism, which is an important factor for the initialization of the combustion process in the case of dual fuel combustion. Further investigations will be carried out to evaluate the mechanisms capability to describe the ignition in presence of natural gas and the premixed combustion in the lean gas-air mixture, which are typical for dual fuel combustion processes. The generated model will be transferred to a model of a single cylinder research engine to investigate the kinetically controlled processes of knocking and flame quenching, which limit the combustion process. Thereby, large eddy simulation will be applied to study the cycle-to-cycle variations.

REFERENCES

- [1] International Maritime Organization MARPOL, *Annex VI. Regulations for the prevention of air pollution from ships and the NOx Technical Code*. (2008).
- [2] International Maritime Organization, *Resolution MEPC.175(58) - Amendments to the Annex of the Protocol of 1997 to amend the international Convention for the prevention of pollution from ship, 1973, as modified by the protocol of 1978 relating thereto*. (2008).
- [3] Schlemmer-Kelling U., Bergmann D., Heuser P., *How Legislation Bodies and Customers Influence Maritime Development*. MTZ Industrial (2017) **2**.
- [4] Pischinger S., *How legislation and customer needs drive innovation*. 4. Rostocker Großmotorentagung, Rostock, Germany, (2016).
- [5] Karim G. A., *Dual-Fuel Diesel Engines*. CRC Press, Boca Raton, (2015).
- [6] Kiesling C., Redtenbacher C., Kirsten M., Wimmer A., *Detailed Assessment of an Advanced Wide Range Diesel Injector for Dual Fuel Operation of Large Engines*. CIMAC Congress Helsinki 2016, Helsinki, Finland, June 6-10, (2016).
- [7] Eder L., Ban M., Pirker G., Vujanovic M., *Development and Validation of 3D-CFD Injection and Combustion Models for Dual Fuel Combustion in Diesel Ignited Large Gas Engines*. Energies (2018) **11**:643, doi: 10.3390/en11030643.
- [8] Riess S., Weiss L., Peter A., Rezaei J. et al., *Air Entrainment and Mixture Distribution in Diesel Sprays Investigated by Optical Measurement Techniques*. International Journal of Engine Research, (2017) **19** 1 120-133, doi: 10.1177/1468087417742527.
- [9] Riess S., Vogel T., Wensing M., *Influence of Exhaust Gas Recirculation on Ignition and Combustion of Diesel Fuel under Engine Conditions Investigated by Chemical Luminescence*. 13th Triennial Conference on Liquid Atomization and Spray Systems (ICLASS 2015), Tainan, Taiwan, August 23-27, (2015).
- [10] AVL, *CFD Solver User Guide AVL FIRE VERSION 2017*. (2017).
- [11] Kahila H., Wehrfritz A., Kaario O., Masouleh M. G., *Large-eddy simulation on the influence of injection pressure in reacting Spray A*. Combustion and Flame (2018) **191** 142-159.
- [12] Stiesch G., *Modeling Engine Spray and Combustion Processes*. Springer-Verlag Berlin Heidelberg, (2003), doi: 10.1007/978-3-662-08790-9.
- [13] Dukowicz J., *Quasi-Steady Droplet Phase Change in the Presence of Convection*. Los Alamos Scientific Laboratory, (1979).
- [14] Liu A. B., Mather D., Reitz, R. D., *Modeling the Effects of Drop Drag and Breakup on Fuel Sprays*. SAE Technical Paper 930072, (1993).
- [15] Naber J. D., Siebers D. L., *Effects of Gas Density and Vaporization on Penetration and*

- Dispersion of Diesel Sprays*. SAE Technical Paper 960034, (1996).
- [16] Desantes J. M., Payri R., Salvador F. J., Gil A., *Development and validation of a theoretical model for diesel spray penetration*. *Fuel* (2006) **85** 910-917.
- [17] AVL, *General Gas Phase Reactions Module AVL FIRE VERSION 2017*. 2017.
- [18] Ritzke J., Andree S., Theile M., Henke B. et al., *Simulation of a Dual-Fuel Large Marine Engines using combined 0/1-D and 3-D Approaches*. CIMAC Congress Helsinki 2016, Helsinki, Finland, June 6-10, (2016).

ACKNOWLEDGMENTS

The authors would like to gratefully mention the funding of the project by the *Ministry for Transport, Innovation and Technology* (BMVIT) and the *Austrian Research Promotion Agency* (FFG) in the framework of the *Bridge 1*-program.